Soft Matter

Accepted Manuscript

ROYAL SOCIETY OF CHEMISTRY

www.rsc.org/softmatter

Cite this: DOI: 10.1039/c0xx00000x

www.rsc.org/xxxxxx

ARTICLE TYPE

Into the polymer brush regime through the "grafting-to" method: Densely polymer-grafted rodlike viruses with an unusual nematic liquid crystal behavior

Tingting Zan[a], Fengchi Wu[c], Xiaodong Pei[b], Shaoyi Jia[a], Ran Zhang[a], Songhai Wu*[a], Zhongwei Niu*[c] and Zhenkun Zhang*[b]

Received (in XXX, XXX) Xth XXXXXXXXX 20XX, Accepted Xth XXXXXXXXX 20XX
DOI: 10.1039/b000000x

The current work reports an intriguing discovery of how the force exerted on protein complexes like filamentous viruses by the strong interchain repulsion of polymer brushes can induce subtle changes of the constituent subunits at the molecular scale. Such changes transform into the macroscopic rearrangement of the chiral ordering of the rodlike virus in three dimensions. For this, a straightforward "grafting-to" PEGylation method has been developed to densely graft a filamentous virus with poly(ethylene glycol) (PEG). The grafting density is so high that PEGs are in the polymer brush regime, resulting in straight and thick rodlike particles with a thin viral backbone. Scission of the densely PEGylated viruses into fragments was observed due to the steric repulsion of the PEG brush, as facilitated by adsorption onto a mica surface. The high grafting density of PEG endows the virus with an isotropic–nematic (I-N) liquid crystal (LC) phase transition that is independent of the ionic strength and the densely PEGylated viruses enter into the nematic LC phase at much lower virus concentrations. Most importantly, while the intact virus and the one grafted with PEG of low grafting density can form a chiral nematic LC phase, the densely PEGylated viruses only form a pure nematic LC phase. This can be traced back to the secondary to tertiary structural change of the major coat protein of the virus, driven by the steric repulsion of the PEG brush. Quantitative parameters charactering the conformation of the grafted PEG derived from the grafting density or the I-N LC transition are elegantly consistent with the theoretical prediction.

Introduction

Bioconjugates, formed by covalently grafting synthetic polymers to biomolecules such as proteins, have attracted increasing interest since such marriage can combine the best from both sides which are valuable for biomedicines and many other fields.[1, 2] Some of the best-known bioconjugates, i.e. proteins grafted with polyethylene glycol (PEG) through a process called as PEGylation, have been in clinical applications.[3-5] Besides simple biomolecules, natural protein complexes such as viruses, which consist of more than hundreds of proteins, have also been subjected to polymer grafting in recent years, stimulated by such potential applications as cargo delivery systems for targeting cancer therapy, versatile sensors or diagnostic imaging agents and building blocks for nanomaterials, etc.[6-11]

There are several methods to graft biological objects with polymers, each with its own strength and weakness.[12, 13] In some cases, like PEGylation, the "grafting-to" method seems the only choice while many other polymers can be directly grafted from the biological objects with pre-installed initiators.[4, 12] Normally, one biomolecule can be grafted with only a few copies of polymers. In contrast, the large surface area and multiple copies of the surface functional groups of protein complexes like the viruses offer the possibility to tune the grafting density.[6-11] However, achieving high grafting density of PEG through the "grafting-to" PEGylation method is challenging due to the steric hindrance effect, through which a grafted polymer will prevent its surrounding grafting points from being accessed by other free polymers. Previous pursuits of densely PEGylated viruses normally involved elaborate pre-chemical modifications which might perturb the structural stabilities of the native viruses.[14]

In the current contribution, we report a straightforward method to graft a filamentous virus with several thousand copies of PEG which are in the polymer brush regime (Scheme 1). Pushing the grafted polymers on protein complexes like the viruses into the polymer brush regime has multifaceted significances. First of all, it can be addressed that how the steric repulsion of the polymer brush influence the structural integrity of a virus which consists of many copies of protein subunits largely hold together by non-covalent interactions. Such property is critical in the stability of polymer grafted viruses when circulating in the blood and as the backbone of hybrid materials.[8, 10] Recent works by Xu's group have indicated that the tertiary structure of the α-helical bundles consisting of several α-helical coiled-coil peptides are not perturbed when grafting with very low number of PEG.[15, 16] Whether or not this is true for the case of high number of PEG is an open question.[17] In addition, in the case of filamentous viruses

with a diameter of a few nm, a thin virus-based backbone with a densely grafted polymer brush layer and size monodispersity is the ideal model system for molecular bottlebrushes and wormlike polymeric micelles. Some solution properties, such as the lyotropic liquid phase behavior of these latter two objects are largely uninvestigated due to shortage of well-controlled samples.[15] In this work, the PEG brush will be demonstrated to influence the structural integrity, conformation of the whole virus and also the three dimensional arrangement of the rod-like virus in the nematic liquid crystal (LC) phase. All these changes can be traced back to the secondary to tertiary structural change of the major coat protein of the virus, driven by the steric repulsion of the PEG brush.

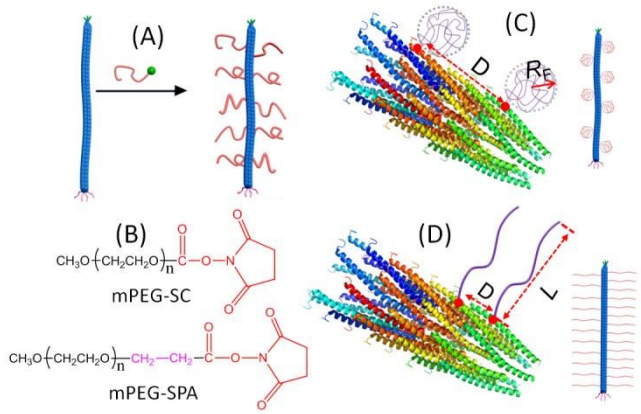

Scheme 1 Schematic illustration of PEGylation of the rodlike *fd* virus (A), the two kinds of PEG used in the current work (B), and the conformation of PEG in the "mushroom" (C) and polymer brush (D) regime, respectively (not to scale). For the sake of clarity, only two PEG chains are shown in the *fd* model (drawn by PyMOL based on the PDB ID code 2MJZ).

Experimental

Materials

Most of the chemicals were obtained from either Sigma-Aldrich or J&K Company and used without any further purification. Water from a Millipore Milli-Q10 system (>18.2 MU) was used. The *fd* virus was grown and purified following the standard biochemical protocol using the XL1-Blue strain of *E. coli* as the host bacteria. *N*-hydroxysuccinimide(NHS)-activated monomethoxy-terminated poly(ethylene glycol) (mPEG-NHS) with a molecular weight of 5000Da and a PDI of 1.01 was purchased from Sinopeg (Xiamen, China) and used as received. Unless otherwise noted, the Tris-HCl buffer (20mM Tris and adjusted the pH by HCl) was used as the standard buffer. The ionic strength of the buffer was adjusted by adding various amounts of NaCl. The concentration of the virus was determined by ultraviolet (UV) absorbance spectroscopy on a UV-2550 UV−vis spectrophotometer (Shimadzu, Japan). The specific absorbance coefficient was 3.84 cm^2 mg^{-1} at 269 nm for the *fd* virus.

Grafting the *fd* virus with PEG

mPEG-NHS in anhydrous DMSO was first prepared (202.50 mg mPEG-NHS dissolved in 100 µL DMSO). The virus was dispersed in PBS buffer (0.01 M, pH 7.8) to form suspensions with a concentration of 1 mg mL^{-1}. mPEG-NHS in DMSO (100 µL) was added to 400 µL the virus suspension. The mixture was stirred at 4 ℃ for 12 h. The excess mPEG-NHS was removed by ultracentrifugation at 55000 rpm for about 6 h followed by dispersing in PBS buffer. Such procedure was repeated three times. After this, the PEGylated virus in PBS buffer was dialyzed against PBS buffer at 4 ℃ for 96 h, with the dialysis buffer changed every 12h. The complete remove of PEG was confirmed by subjecting the PEGylated virus to the AFM check.

Estimation of the Number of PEGs on the surface of each virus

The refractive index increment difference (*dn/dc*) between the bare virus and the one grafted with PEG can be used to estimate the number of grafted polymers on each virus.[19] This is based on the fact that *dn/dc* is proportional to the mass density and the *dn/dc* difference between the bare virus and the one grafted with PEG is due to the grafted polymers. For this, the *dn/dc* of PEG ($(dn/dc)_p$) and the virus ($(dn/dc)_{fd}$) were determined on an Optilab DSP interferometric refractometer (Wyatt Technology, USA) at T = 25°C and the wavelength = 632 nm. The number of PEG grafted on each virus, *N*, can be estimated by the following equation:

$$N = \frac{(dn/dc)_{app} - (dn/dc)_{fd}}{(dn/dc)_p} \times \frac{M_w^{fd}}{M_w^p}$$

Where M_w^{fd} and M_w^p the molecular weight of the *fd* virus (1.64 × 10^7 g mol^{-1}) and of PEG (5000), respectively. $(dn/dc)_{app}$ refers to apparent *dn/dc* of the PEG grafted virus since the concentration of the virus suspensions can be easily obtained by UV absorption (PEG does not absorb in the UV range where the *fd* virus absorbs). Several virus suspensions with concentrations in the range of from 0.001 to 0.005 g mL^{-1} in pure water were prepared for PEG, the *fd* virus and PEG grafted virus. The *dn/dc* values of 0.39, 0. 20 and 0.17 mL g^{-1} are obtained for *fd*-SC, PEG, and *fd*, respectively. With the above equation, $N \sim 3500$ is calculated.

Atomic Force Microscopy of the (PEGylated) viruses

For the atomic force microscopy (AFM), the (PEGylated) viruses were dialyzed against ultrapure water for at least three days to remove any trace of PEG and salts. Drops of virus suspension of 0.01 mg mL^{-1} were then delivered to a fresh-cleaved mica surface and dried. The AFM observation was performed by the tapping mode on a NanoScopeR IIIa (Veeco) AFM system, with an etched silicon tip (RTESP, Bruker; spring constant k = 40 N/m; frequency f_0 = 300 kHz). Image processing was performed with NanoScope 5.31r1 software.

Circular Dichroism Measurements of the (PEGylated) viruses

Circular dichroism (CD) spectra were recorded on a MOS-500 circular dichroism spectrophotometer (Bio-Logic, France) in the wavelength range of 200-260 nm. The virus sample was suspended in Tris-HCl buffer (5 mM, pH 8.2). Data were collected using quartz cuvettes with a 2 mm path length (Starna). The samples were diluted to 0.08 mg mL^{-1}. The temperature was controlled using a thermostat water bath.

Fluorescence measurement

Intrinsic Fluorescence of the Tryptophan Residue (W26) of pVIII. Measurements of the intrinsic fluorescence spectra of the (PEGylated) viruses due to the tryptophan residual at the position of 26 of the pVIII coat protein were conducted with a HITACHI (F-4600). The samples were dispersed into Tris-HCl (pH 8.2, 5 mM) buffer with a concentration of 3 mg mL^{-1}. The excitation wavelength was set to 295 nm and the bandwidths for excitation and emission were set at 2.5 and 5.0 nm, respectively.

1-Anilino-8-naphthalenesulfonate (ANS) Fluorescence. Measurements of the ANS fluorescence spectra of the (PEGylated) viruses were conducted with a HITACHI (F-4600). A stock ANS solution in ethanol with a concentration of 2 mg mL^{-1} was freshly prepared. The ANS stock solution (10 μL) was added to 1 mL (PEGylated) virus samples with a concentration of 3 mg mL^{-1} and the mixture was incubated for 30 mins before recording the corresponding fluorescent spectra. The excitation wavelength was set to 345 nm and the scan wavelength was between 370 and 670 nm, the excitation and emission slit were set at 5.0 and 10.0 nm, respectively.

SDS-PAGE of the (PEGylated) Viruses

Sodium dodecyl sulfate (SDS)-polyacrylamide gel electrophoresis (SDS-PAGE) was performed following Laemmli's method. The (PEGylated) viruses were denatured in a buffer containing 1.6% (w/v) SDS, 1% (v/v) *β*-mercaptoethanol, 12.5% (v/v) glycerol, 0.0025% (w/v) bromophenol blue, and 50 mM Tris (pH 7.6) (final concentration). The resulting mixture of capsid proteins, and other agents was loaded onto a 16% urea gel. Usually, 20 μg of virus was used. Commercially available molecular-weight markers (SeeBlueR Plus2) were applied to one lane of each gel. Gels were stained with Coomassie Brilliant Blue R-250 in order to visualize the protein bands. The capsid protein pVIII is the dominant protein and is intensely stained.

MALTI-TOF MS of the PEGylated Viruses

The PEGylated viruses were first dissembled by adding 6 μL guanidinium chloride (6M) to 24 μL PEGylated viruses and incubating for 5 mins at room temperature. The salts in the mixture were removed by filtering through a Millipore $ZipTip_{\mu}$-C18 tip, with a mixture of TFA (0.1%) and ACN (50 %) as the eluent. The pVIII was spotted onto a MALDI plate using sinapic acid as the matrix and analyzed on a MALDI-TOF AutoflexIII LRF200-CID mass spectrometer (Bruker).

Dynamic light scattering

The average hydrodynamic diameters of the PEGylated viruses in suspension state were obtained by dynamic light scattering on a laser light scattering goniometer (BI-200SM) equipped with a digital correlator (BI-10000AT) and a laser source of 532 nm. All of the samples were centrifuged at 5000 g at 4 °C in order to remove dust right before characterization. The concentration of the virus was 6.0×10^{-5} mg mL^{-1}, well below the overlap concentration. Data were collected at a scattering angle of 30 °.

Liquid-Crystalline Behaviors of the (PEGylated) Viruses

To investigate the isotropic–nematic (I-N) liquid crystal phase transition of the (PEGylated) viruses, all (PEGylated) viruses were purified and dispersed in Tris–HCl buffer (pH 8.2, the ionic strength was adjusted by adding NaCl), resulting in concentrated suspensions in the nematic LC phase with clear birefringence while observing through crossed polarizers. The suspension was diluted to the coexistence region at the I–N transition by adding the same buffer. The concentration was measured in such a sample and was taken as the phase transition concentration, $C_{I\text{-}N}$.

To reveal the nature of the (chiral) nematic LC phase of the (PEGylated) virus, concentrated virus stock suspensions with a concentration deep in the nematic phase range were prepared. Decades of μL samples was filled into 1.5 mm glass capillaries, flame sealed and checked on an Olympus BX41 polarized optical microscope (POM) equipped with an LMPLanFL N lens (Olympus, LMPLanFL N) and recorded with a CCD camera (Micropublisher, 3.3RTV). The glass capillaries were cleaned with chromic acid and repeatedly rinsed with deionized water. Several capillaries containing the same samples were prepared at the same time to exclude any potential influence of the inner surface of the capillary. The sealed capillaries containing the virus samples were stored at 4 ℃ and checked with POM for more than six months.

Results and Discussion

PEGylation of rodlike viruses via the "grafting-to" method

For the current work, we chose a filamentous bacteriophage-the *fd* virus with a rod-like shape of a length of 880 nm and a diameter of 6.6 nm.[16] This virus consists of ca. 2700 identical major coat proteins, pVIIIs, which self-assemble in a helical way into a capsid (Scheme 1C). The solvent-exposed portion of pVIII contains rich functional groups such as amino, carboxyl groups which offer tremendous opportunities for chemical modifications.[17, 18] For PEGylation, we used mPEG-SPA and mPEG-SC with a molecular weight of 5k and a narrow molecular weight distribution (Scheme 1B). Both kinds of PEGs are *N*-hydroxysuccinimide (NHS)-activated polymers targeting the surface amino groups of the virus and the only difference between them is the spacer between the NHS group and the main segment of the polymer chain (Scheme 1B).

For PEGylation of the virus, the molar ratio of PEG to the surface amino group of the virus is at least more than 300:1, in order to approach the maximum grafting density. The excess PEG was removed by subjecting the grafted virus suspension to several rounds of centrifugation/redispersion, followed by intensive dialysis. The complete removal of PEG was later confirmed by MALDI-TOF MS and atomic force microscopy (AFM) (Figure S1A in ESI). Hereafter, we refer to the virus grafted with mPEG-SPA and mPEG-SC as the *fd*-SPA and *fd*-SC, respectively.

The two kinds of PEGylated viruses were subjected to denaturized SDS-PAGE and MALDI-TOF MS characterizations (Fig. 1A and S3 in ESI). Under the above mPEG-SC/virus ratio, the band corresponding to the intact pVIII coat protein disappears while two new bands appear: one corresponding to pVIII grafted with one PEG and another pVIII grafted with two PEGs (Fig. 1A). However, in the case of mPEG-SPA, there is always a band corresponding to un-grafted pVIIIs, even after increasing the mPEG-SPA/virus ratio to such a degree that drives the virus to aggregate (Fig. 1A and S3A in ESI). In the MALDI-TOF MS, two peaks appear and the m/z ratio can be ascribed to one pVIII (5238) plus one PEG (5388) or two PEG (10776) (Fig. 1B, C and

D). The number of PEG on each virus is estimated with a reasonable accuracy by the difference of the refractive index increment, *d*n/*d*c, between the pure and PEG grafted virus.[19] In the case of *fd*-SC, there is ca. 3500 PEG chains per virus while 1000 PEG chains per virus can be achieved in the case of *fd*-SPA under the highest polymer/virus ratio that can be accessed. For both kinds of PEG, the grafting density is much higher than those reported in previous works.[19, 20] The large amount of excess PEG used in this work may exert the crowding effect to facilitate the interaction of PEG with the virus surface, similar to a recent report in which polymeric depletants were used to enhance the PEG grafting density on the surface of some cells.[21] The different grafting density under identical conditions achieved with the two kinds of PEG can be attributed to the spacer difference (Scheme 1B). mPEG-SPA becomes popular in PEGylation due to the increasing stability against hydrolyzation of the NHS group.[4] The two methylenes between the amino-active NHS group and the main segment of this PEG offer the steric hindrance to constrain the NHS group from attacking by water or the surface amino groups of the virus. In contrast, such steric hindrance is much weaker in the case of mPEG-SC since the NHS group is directly connected to the PEG backbone.

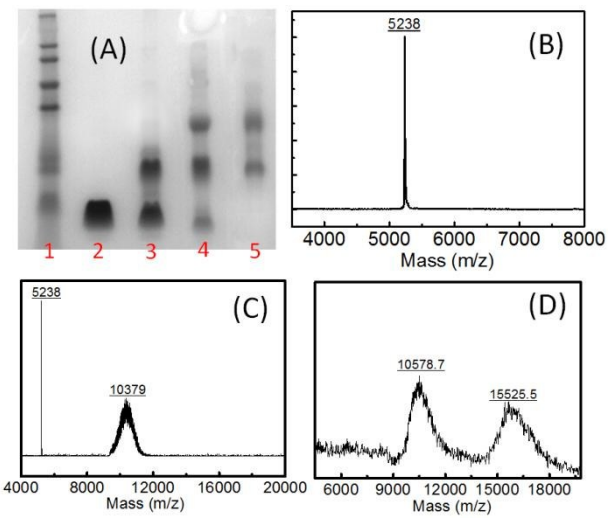

Fig. 1 SDS-PAGE (A) and MALDI-TOF MS (B, C and D) analysis of the (PEGylated) *fd* viruses. Lane 1 in (A): Marker; Lane 2 in (A) and MS in (B): pure virus; Lane 3 in (A) and MS in (C): *fd* virus grafted with 400 PEG per virus; Lane 4 in (A): *fd* virus grafted with mPEG-SPA; Lane 5 in (A) and MS in (D): *fd* virus grafted with mPEG-SC.

By assuming the grafted PEG chains homogeneously distribute around the virus surface, the conformation of the PEG chains can be estimated, based on the Flory dimension (R_F) of the grafted PEG, the distance between grafting points (D) (Scheme 1C and D, also see ESI for the detailed discussion).[10] In the case of *fd*-SC, each pVIII is grafted with at least one PEG chain. For a biological nanoplatform like the virus, the advantage is that the inter-distance of the amino groups (*N*-terminal and lysine at the position of 6), i.e. the grafting point of the PEG chains (D), can be accurately calculated in the range of 1 to 2.40 nm.[22] The Flory dimension (R_F) of PEG with a molecular weight 5k (PEG5k) is 6 nm (See ESI). Therefore, D is less than the R_F and the PEG chains on the surface of *fd*-SC are in the polymer brush regime.[23] In the case of the *fd* virus grafted with 400 PEG, as typically achieved in previous works,[19, 20] the inter-distance of the anchor points is in the range of 10.80 to 16.20 nm, which is larger than R_F of PEG5k. Therefore, the PEG chains are in the "mushroom" regime.

Scission of the Densely PEGylated virus on a mica surface

The PEGylated *fd* viruses were checked with AFM, together with the pertinent virus. First of all, there is no detectable PEG in the system, suggesting the successful removal of the excess PEG since this polymer has high propensity to crystallize and can be easily detected by AFM (Fig. S1A in ESI). While the pertinent virus and the one grafted with 400 PEG per virus appear as rod-like particles with either a curved or straight conformation (Fig. 2A), the densely PEGylated *fd*-SC presents itself as a thick and straight rodlike conformation (Fig. 2B and D) and has increased tendency to form ordering structure during solvent evaporation (Inset in Fig. 2B). The apparent thickness of different *fd*-SC from the section analysis is constant, suggesting the PEGylation of each virus is homogeneous (Fig. S2 in ESI). A mixture of the pertinent virus and *fd*-SC was investigated by AFM to exclude any influence from the preparation conditions (Fig. 1D and S1B in ESI). From the section analysis, the relative surface and horizontal diameters of the two kinds of viruses can be estimated: *fd*-SC is three times larger than the pure virus in terms of both values.

Another distinct feature is that, although most of the original *fd* virus or these grafted with ca. 400 PEG per virus have a classical length of 880 nm, there are many short and thick rods with various lengths that is much less than 880 nm in the case of the *fd*-SC (Fig. 2B and Fig.S1D in ESI). Statistics of more than 100 particles further suggests such length polydispersity (Fig. 2C). We believe that the short rods should be fragments of the parent viruses. The lateral pressure exerted on the virus due to interchain repulsion of the grafted PEG chain is estimated based on the well-established theory of lipid membrane that grafted with PEG (See the ESI for the detailed calculation).[24] The lateral pressure with a value in the range of 2.28 ~ 3.45 mN m^{-2} is estimated based on the grafting density of ca. 3500 PEG per virus. Such value is well beyond the forces that induce the straightening of the same rodlike virus during physical stretching as demonstrated in previous works.[25, 26] Therefore, the rodlike *fd*-SC becomes less flexible and is vulnerable to shearing distortion during the evaporation of the solvent. Such interactions, as facilitated by adsorption onto the mica surface, were also suggested as the origin of scission of the carbon-carbon bond of the main chain of some molecular bottlebrushes.[27, 28] Compared to the covalent bond, the virus is hold together by the hydrophobic stacking of the central portion of the pVIII coat proteins and electrostatic interactions of the C-terminal of pVIII with the encapsulated DNA.[29] Therefore, the inter-chain steric repulsion of the grafted PEG brush should be enough to break the virus into fragments, as facilitated by the adsorption on to the mica surface during evaporation. However, dynamic light scattering of the virus in the suspension state reveals that all kinds of viruses have a similar apparent hydrodynamic diameter that equivalent to a sphere created by the rotational diffusion of the rodlike virus (Fig. S4 in ESI). Therefore, fragmentation mainly occurs at the solid mica surface.

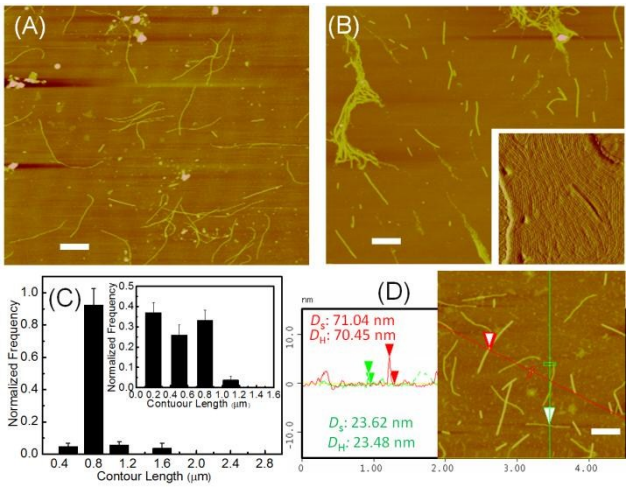

Fig. 2 Atomic force microscopy of the (PEGylated) *fd* viruses. (A) Mixture of the *fd* virus and the one grafted with 400 PEG per virus. (B) *fd* virus grafted with PEG through mPEG-SC to approach the maximum grafting density (*fd*-SC). Inset: an ordered structure formed by many *fd*-SC. (C) Distribution of the contour length of the virus in (A). Inset: the virus in (B). (D) Section analysis of the mixture of the *fd* virus and *fd*-SC. DS and DH refer to the surface and horizontal diameter, respectively. Scale bar: 400 nm.

Liquid crystal (LC) behaviors of densely PEGylated virus

Due to its size monodispersity and high aspect ratio, the *fd* virus is a perfect colloidal rod that has been used to test Onsager theory of the isotropic-nematic (I-N) LC phase transition of rodlike particles upon increasing the particle concentration.[30] The liquid crystal (LC) behavior of the pristine *fd* virus, the one grafted with 400 PEG on each virus and the densely PEGylated virus (*fd*-SC) were compared (Fig. 3). The LC behavior of the former two has been well-established and follows $n\pi L^2 D_{eff} \cong 16$, where n is the number density of the virus at the I-N transition and D_{eff} is the effective diameter of the virus.[19] The *fd* virus is highly charged and D_{eff} is determined by the electric double layer (EDL).[19] With increasing ionic strength (I), the EDL is compressed and D_{eff} decreases, the virus concentration at the I-N transition, $C_{I\text{-}N}$, increases (Fig. 3A). The *fd* virus grafted with 400 PEG on its surface, has such dependency at low I, but becomes roughly independent of I at $I \geq 50$ mM, above which the EDL is confined into the PEG layer (Fig. 3C). However, in the case of *fd*-SC, the I-N transition is independent of I in the whole I and $C_{I\text{-}N}$ shifts to a much lower virus concentration. It can be rationalized that PEGs in the polymer brush range extend themselves from the virus surface. The EDL even at very low I is well confined inside the PEG layer (Fig. 3C). Therefore, the inter-particle interaction is dominated by the PEG layer in the whole range of the ionic strength.

As listed in Figure 3B, the D_{eff} at several ionic strengths can be estimated by the concentration at the I-N transition.[19] In the whole ionic strength range, the *fd*-SC has an average diameter of 30 nm. Since the diameter of the bare *fd* virus is 6.6 nm, the thickness of the PEG layer (L) is 12 nm. This value is less than the contour length of 30 nm of a fully stretched PEG of a Mw 5k, but is much larger than PEG with a coiled globule conformation of a size of $2R_g \sim 6$ nm (R_g, the radius of gyration, is ca. 3 nm for PEG5k). More importantly, this value is very close to the maximum extension length of the grafted PEG5k from the surface, as predicted by the de Gennes analysis.[31] These estimations are also consistent with the very recent results of simulations about PEGs grafted on a single-walled carbon nanotubes.[32] In addition, at I = 110 nm, D_{eff} of the bare *fd* is close to 7 nm.[19] Therefore, the ratio of D_{eff} of *fd*-SC to the bare *fd* is ca. 4, which is consistent with the height ratio estimated from AFM (Fig. 2D). Altogether, *fd*-SC with densely grafted PEG in the polymer brush range becomes a completely sterically stabilized system and its I-N transition is independent of the ionic strength.

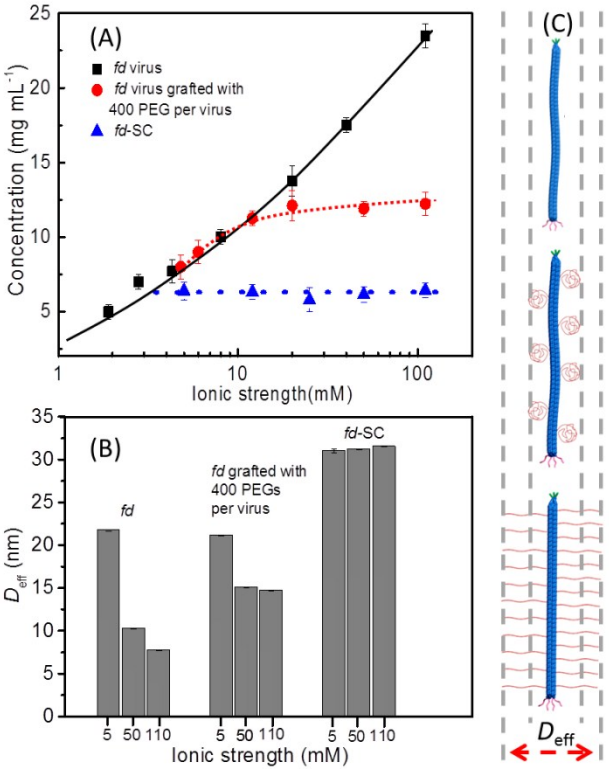

Fig. 3 Liquid crystal (LC) behavior of the (PEGylated) *fd* viruses. (A) Isotropic-nematic (I-N) LC phase transition at varied ionic strengths (I). (B) Effective diameter (D_{eff}) at I = 5, 50 and 110 mM as estimated from the corresponding concentration at the I-N LC transition. (C) Schematics of the double layer at several ionic strengths for the three kinds of viruses listed in (B). From the top to bottom: *fd* virus, *fd* grafted with 400 PEG per virus and *fd*-SC.

Nature of the nematic liquid crystal phase of the densely PEGylated virus

One of the unique properties of the *fd* virus is that it indeed forms a chiral nematic LC (CLC) phase above the I-N transition in which the virus rotates around a given director, resulting in stripe-like fingerprint textures.[33] Grelet and Fraden have shown that the *fd* virus grafted with ca. 400 PEG5k per virus can still form the CLC phase.[19] The nature of the nematic LC phase of the *fd*-SC with densely grafted PEG5k was also investigated. While the intact *fd* virus and the one grafted with ca. 400 PEG5k per virus form the CLC phase, no typical feature due to the CLC phase appears in the case of *fd*-SC even after more than 6 month under the identical conditions (Fig. 4). Therefore, the *fd*-SC is believed to only form a pure nematic LC phase. This is the first example that the three dimensional arrangements of the rod-like particles can be influenced by pushing the grafted polymers into the brush regime.

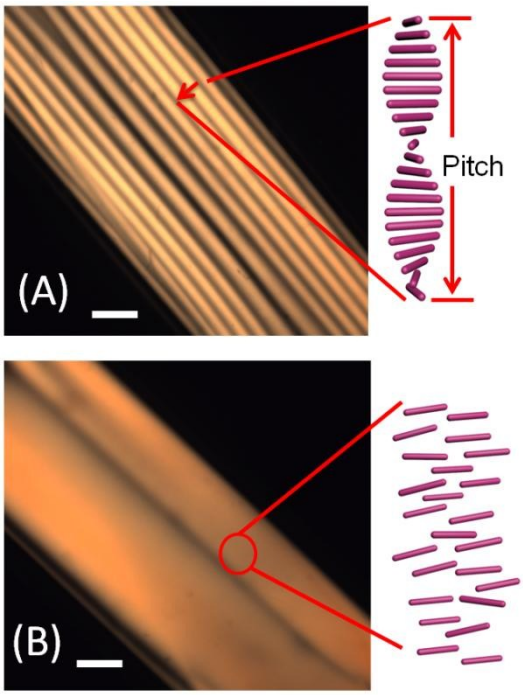

Fig. 4 Nature of the nematic liquid crystal (LC) phase behavior of the (PEGylated) viruses. (A) A chiral LC phase observed with the *fd* virus grafted with 400 PEG per virus. (B) A pure nematic LC phase observed with *fd*-SC. The concentration in (A) and (B) is 16 mg mL^{-1} in Tris buffer with *I* = 110 mM and pH = 8.2. Scale bar: 100 μm.

The microscopic origin of macroscopic chirality of the fd virus is an unanswered question, as exampled by a recent simulation.[45] A superhelical conformation assumption has been suggested as the origin of the CLC phase of rodlike viruses.[19, 34] In this assumption, some viruses like the *fd*, might exist as a dynamic "corkscrew" shape in solution. Whether or not a virus adopts such conformation is probably determined by the interaction of the encapsulated DNA and the major coat proteins.[35] There is mounting evidence that supports such assumption and recent results also demonstrate that the superhelical conformation can be further influenced by chemical modifications and temperature, etc.[36,37] To understand the underlying mechanism of the nematic LC phase behaviour of *fd*-SC, the three kinds of viruses was subjected to the scrutiny of several biophysical methods which sense different levels of structural changes of the major coat protein (pVIII), ca. 2700 copies of which constitutes the cylindrical capsid of the *fd* virus (Scheme 1C).[37]

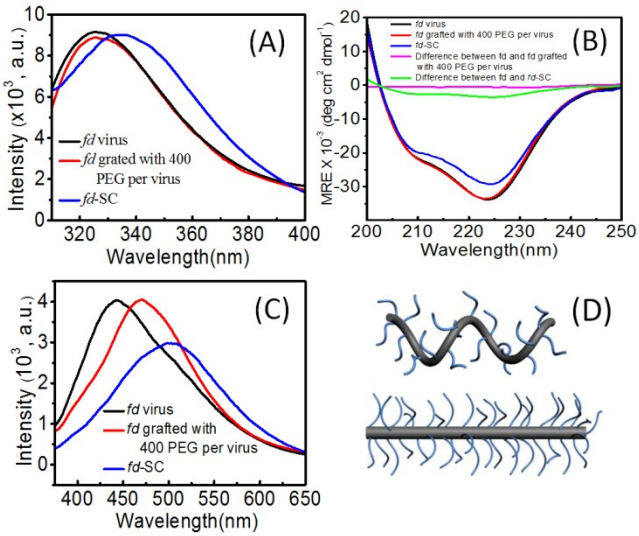

Fig. 5 Spectroscopic method to reveal structural changes at various scales induced by PEGylation. (A), (B) and (C) are the intrinsic fluorescence of the amino acid residual at the position of 26 (W26), CD of pVIII and ANS fluorescence of the three kinds of viruses as listed in Figure 3B, respectively. (D) Possible conformations of the *fd* virus at various grafting density of PEG.

The intrinsic fluorescence of the tryptophan residue (W26) was first investigated (Fig. 5A).[38] W26 locates in the middle of the hydrophobic section of pVIII that is responsive for the inter-subunit packing of pVIII in the capsid.[39] Pronounced red-shift occurs to the fluorescent emission spectra of *fd*-SC while the intact *fd* virus and the one grafted with 400 PEGs per virus are similar to each other. The red-shift indicates the local microenvironment surrounding the W26 residue become more hydrophilic, due to the slightly unwinding of the alpha-helix of pVIII. The secondary structure of pVIII was assessed by circular dichroism (CD) (Fig. 5B). The CD signals of *fd*-SC decreases while the *fd* virus and these grafted with 400 PEGs per virus are identical with each other. Estimation reveals that the α-helical content of pVIII of the *fd*-SC decreases to 86% from 96% of the other two kinds of viruses.[40] Finally, the change of the inter-subunit packing of the pVIII inside the viral capsid was detected by the 1-Anilino-8-naphthalenesulfonate (ANS) fluorescence (Fig. 5C). While in the non-fluorescent state in aqueous solution, ANS emits strong fluorescence by penetrating into the hydrophobic domains of the inter-subunit in the viral capsid.[37] The emission peak of the ANS fluorescence of the virus grafted with 400 PEG per virus shifted to a longer wavelength than that of the intact *fd* virus while the intensity is the same. The red-shift of the ANS fluorescence in the case of PEGylated viruses suggests the local environment of ANS become more hydrophilic, due to the hydration of the grafted PEG which can bound to many water molecules.[41] However, such hydration alone cannot explain the intensity decrease and strong red-shift that simultaneously occurred to *fd*-SC. Together with the distinct behaviour of *fd*-SC in terms of the intrinsic fluorescence of W26 and CD of pVIII, it can be concluded that steric interactions of the PEG brush produce stress enough to promote unwinding of pVIII and changing of its packing style in the capsid. Such change might force *fd*-SC to deviate from the dynamic "corkscrew" shape in suspension (Fig. 5D). This is consistent with the decreasing

flexibility as revealed by the thick and straight conformation in AFM. It is noted here that mechanical force within the polymer brushes have been immerging as a versatile means to break chemical bonds (mechochemistry), to change membrane rigidity and to change the shape of macroscopic materials.[42-44]

Conclusions

In summary, by decreasing the steric effect of the spacer between the NHS and PEG main chain, we success in densely grafting the rodlike *fd* virus with PEG of Mw 5k. The degree of grafting density is so high that the PEG chains are in the brush regime. Such a highly densely grafted virus has a thick and straight conformation. Scission of the otherwise stable virus is observed which can be attributed to the strong steric interaction among PEG brushes and the adsorption effect on the mica surface. Most importantly, the high grafting density endows the virus with isotropic–nematic phase transition that is independent of ionic strength and the densely PEGylated virus enters into nematic phase at much lower concentration. From a molecular level, the steric repulsion interactions of the PEG brush disturb the secondary and tertiary structure of the pVIII coat protein and force the virus in suspension to deviate from an assumed "corkscrew" conformation, which might be the reason behind the fact that densely PEGylated virus can only form a pure nematic LC phase.

Acknowledgment

This work was supported by the National Natural Science Foundation of China (No. 21274067, 91127045, 51390483), the Fundamental Research Funds for the Central Universities, Natural Science Foundation of Tianjin, China (No. 12JCQNJC01800) and PCSIRT (IRT1257). Z.Z.K thanks Prof. Linqi Shi for his generous supporting.

Notes and references

[a] *School of Chemical Engineering and Technology, Tianjin University, Tianjin 300072, China Tel: 0086-22-87401961; E-mail:* wusonghai@tju.edu.cn

[b] *Key Laboratory of Functional Polymer Materials of Ministry of Education, Institute of Polymer Chemistry, College of Chemistry, Nankai University, Tianjin 300071, China Tel: 0086-22-23501945; E-mail:* zkzhang@nankai.edu.cn

[c] *Key Laboratory of Photochemical Conversion and Optoelectronic Materials, Technical Institute of Physics and Chemistry, Chinese Academy of Sciences, Beijing 100190, China. Tel: 0086-010-82543429; E-mail:* niu@mail.ipc.ac.cn

† Electronic Supplementary Information (ESI) available: Estimation of the conformation of the PEG chains on the virus surface and supplementary figures. See DOI: 10.1039/b000000x/

1. J. Y. Shu, B. Panganiban and T. Xu, *Annu. Rev. Phys. Chem.*, 2013, **64**, 631-657.
2. L. A. Canalle, D. W. Löwik and J. C. van Hest, *Chem. Soc. Rev.*, 2010, **39**, 329-353.
3. J. M. Harris and R. B. Chess, *Nature Reviews Drug Discovery*, 2003, **2**, 214-221.
4. M. Roberts, M. Bentley and J. Harris, *Adv. Drug Del. Rev.*, 2012, **64**, 116-127.
5. E. M. Pelegri-O'Day, E.-W. Lin and H. D. Maynard, J. *Am. Chem. Soc.*, 2014, **136**, 14323-14332.
6. J. K. Pokorski, K. Breitenkamp, L. O. Liepold, S. Qazi and M. Finn, *J. Am. Chem. Soc.*, 2011, **133**, 9242-9245.
7. K. S. Raja, Q. Wang, M. J. Gonzalez, M. Manchester, J. E. Johnson and M. G. Finn, *Biomacromolecules*, 2003, **4**, 472-476.
8. M. Z. Tesfay, A. C. Kirk, E. M. Hadac, G. E. Griesmann, M. J. Federspiel, G. N. Barber, S. M. Henry, K.-W. Peng and S. J. Russell, *J. Virol.*, 2013, **87**, 3752-3759.
9. K. D. Fisher, Y. Stallwood, N. K. Green, K. Ulbrich, V. Mautner and L. W. Seymour, *Gene Ther.*, 2001, **8**, 341-348.
10. K. L. Lee, S. Shukla, M. Wu, N. R. Ayat, C. E. El Sanadi, A. M. Wen, J. F. Edelbrock, J. K. Pokorski, U. Commandeur, G. R. Dubyak and N. F. Steinmetz, *Acta Biomater.*, 2015, **19**, 166-179.
11. S. S. Gupta, K. S. Raja, E. Kaltgrad, E. Strable and M. G. Finn, *Chem. Commun.*, 2005, 4315-4317.
12. B. S. Sumerlin, *ACS Macro Letters*, 2011, **1**, 141-145.
13. R. M. Broyer, G. N. Grover and H. D. Maynard, *Chem. Commun.*, 2011, **47**, 2212-2226.
14. Z. M. Carrico, M. E. Farkas, Y. Zhou, S. C. Hsiao, J. D. Marks, H. Chokhawala, D. S. Clark and M. B. Francis, *ACS nano*, 2012, **6**, 6675-6680.
15. J. Y. Shu, R. Lund and T. Xu, *Biomacromolecules*, 2012, **13**, 1945-1955.
16. R. Lund, J. Shu and T. Xu, *Macromolecules*, 2013, **46**, 1625-1632.
17. E. Hamed, D. Ma and S. Keten, *ACS Biomaterials Science & Engineering*, 2015, **1**, 79-84.
18. Z. Zhang and E. Grelet, *Soft Matter*, 2013, **9**, 1015-1024.
19. E. Grelet and S. Fraden, *Phys. Rev. Lett.*, 2003, **90**, 19
20. Z. Dogic and S. Fraden, *Philosophical Transactions of the Royal Society of London. Series A: Mathematical, Physical and Engineering Sciences*, 2001, **359**, 997-1015.
21. N. A. Rossi, I. Constantinescu, D. E. Brooks, M. D. Scott and J. N. Kizhakkedathu, *J. Am. Chem. Soc.*, 2010, **132**, 3423-3430.
22. Y. S. Nam, T. Shin, H. Park, A. P. Magyar, K. Choi, G. Fantner, K. A. Nelson and A. M. Belcher, *J. Am. Chem. Soc.*, 2010, **132**, 1462-1463.
23. P. G. de Gennes, *Adv. Colloid Interface Sci.*, 1987, **27**, 189-209.
24. D. Marsh, *Biophys. J.*, 2001, **81**, 2154-2162.
25. A. S. Khalil, J. M. Ferrer, R. R. Brau, S. T. Kottmann, C. J. Noren, M. J. Lang and A. M. Belcher, *Proceedings of the National Academy of Sciences*, 2007, **104**, 4892-4897.
26. D. Alsteens, E. Pesavento, G. Cheuvart, V. Dupres, H. Trabelsi, P. Soumillion and Y. F. Dufrêne, *ACS nano*, 2009, **3**, 3063-3068.
27. S. S. Sheiko, F. C. Sun, A. Randall, D. Shirvanyants, M. Rubinstein, H.-i. Lee and K. Matyjaszewski, *Nature*, 2006, **440**, 191-194.
28. Z. Zheng, M. Müllner, J. Ling and A. H. E. Müller, *ACS Nano*, 2013, **7**, 2284-2291.
29. J. W. Keum, A. P. Hathorne and H. Bermudez, *Wiley Interdisciplinary Reviews: Nanomedicine and Nanobiotechnology*, 2011, **3**, 282-297.
30. Z. Dogic and S. Fraden, *Current Opinion in Colloid & Interface Science*, 2006, **11**, 47-55.
31. A. K. Kenworthy, K. Hristova, D. Needham and T. J. McIntosh, *Biophys. J.*, 1995, **68**, 1921-1936.
32. H. Lee, *The Journal of Physical Chemistry C*, 2013, **117**, 26334-26341.
33. Z. Dogic and S. Fraden, *Langmuir*, 2000, **16**, 7820-7824.
34. E. Barry, D. Beller and Z. Dogic, *Soft Matter*, 2009, **5**, 2563-2570.
35. S. Tomar, M. M. Green and L. A. Day, *J. Am. Chem. Soc.*, 2007, **129**, 3367-3375.
36. J. Cao, S. Liu, J. Xiong, Y. Chen and Z. Zhang, *Chem. Commun.*, 2014, **50**, 10402-10405.
37. S. Liu, T. Zan, S. Chen, X. Pei, H. Li and Z. Zhang, *Langmuir*, 2015, **31**, 6995-7005.
38. G. E. Arnold, L. A. Day and A. K. Dunker, *Biochemistry*, 1992, **31**, 7948-7956.
39. K. L. Aubrey and G. J. Thomas Jr, *Biophys. J.*, 1991, **60**, 1337.
40. B. A. Clack and D. M. Gray, *Biopolymers*, 1989, **28**, 1861-1873.
41. O. Tirosh, Y. Barenholz, J. Katzhendler and A. Priev, *Biophys. J.*, 1998, **74**, 1371-1379.
42. H.-A. Klok and J. Genzer, *ACS Macro Letters*, 2015, **4**, 636-639.
43. Y. Zou, A. Lam, D. E. Brooks, A. Srikantha Phani and J. N. Kizhakkedathu, *Angew. Chem. Int. Ed.*, 2011, **50**, 5116-5119.

44. Z. Lei, S. Yang and E.-Q. Chen, *Soft matter*, 2015, **11**, 1376-1385.
45., S. Dussi, S. Belli, R. van Roij, M. Dijkstra, *J. Chem. Phys.*, 2015, **142**, 074905.

Table of contents:

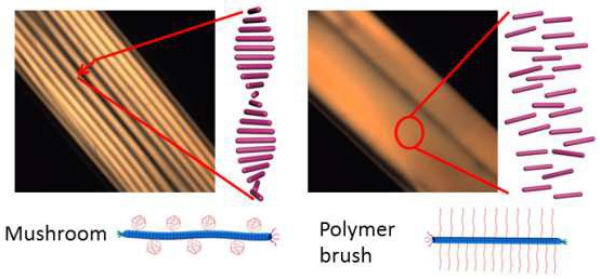

Densely PEGylated rodlike *fd* viruses can only form a pure nematic LC phase. This can be traced back to the secondary to tertiary structural change of the major coat protein of the virus, driven by the steric repulsion of the PEG brush.